Transverse versus Longitudinal Eigenperiods of Multispan Seismically isolated Bridges

Georgios Kampas[1], Nicos Makris[2]

Department of Civil Engineering, University of Patras, GR-26500, Greece

ABSTRACT

This paper is motivated from the wider need in system identification studies to identify and interpret the eigenvalues of seismically isolated bridges from field measurements. The paper examines the transverse eigenvalues of multispan bridges which are isolated in both transverse and longitudinal directions at all supports including all center piers and end-abutments. The paper shows that regardless of the value of the longitudinal isolation period of the deck, the length of the bridge and the number of spans, the first transverse (isolation) period is always longer than the longitudinal isolation period of the deck. This result cannot be captured with the limiting idealization of a beam on continuously distributed springs (beam on Winkler foundation) which yields the opposite result–that the first transverse period is always shorter than the longitudinal isolation period. This fundamental difference between the response of a flexural beam supported on distinct, equally spaced springs and that of a beam supported on continuously distributed springs has not received the attention it deserves in the literature of structural mechanics-dynamics. Finally, the paper shows that the first normalized transverse eigenperiod of any finite-span isolated deck follows a single master curve and the solutions from all configurations are self-similar and are not dependent on the longitudinal isolation period or on whether the deck is isolated on elastomeric or spherical sliding bearings.

Keywords: seismic isolation; bridges; eigenvalues; system identification; self similarity; dynamic response

[1]Doctoral Candidate, Dept. of Civil Engineering, University of Patras, Greece, GR 26500, gkampas@upatras.gr

[2] Professor, Dept. of Civil Engineering, University of Patras, Greece, GR 26500, nmakris@upatras.gr

INTRODUCTION

Traditionally several conventionally designed bridges use elastomeric bearings (pads) between the deck and its supports to accommodate thermal movements. The long experience of bridge engineers with the technology of bearings had a positive role in the implementation of isolation bearings to protect bridges from earthquakes. Seismic isolation, with either elastomeric or sliding bearings, is at present widely adopted as an effective technology for the seismic protection of highway and railway bridges (Skinner et al.1993, FHWA 1995).

In an earlier publication (Makris et al. 2010), the authors examined the eigenvalues of a seismically isolated deck with its ends restricted from translating along the transverse direction (pinned supports at the end-abutments); while, the deck was fully isolated along the longitudinal direction. Restricting the ends of the deck from translating laterally is nearly imperative in railway bridges in order to avoid misalignment of the rails at the deck-abutment joints during earthquake shaking and it was concluded that for isolated bridges longer than a certain length the first transverse isolation period despite the flexural rigidity of the deck is longer than the longitudinal period; this critical length depends on whether the bridge is isolated on elastomeric bearings or on spherical sliding bearings.

In highway bridges there are usually shear keys at the end abutments; however, the gap between the deck and the shear keys may be large enough (5.0 to 8.0cm), so that under small amplitudes of vibration the ends of the deck behave as free ends. This paper complements the work of Makris et al. (2010) and examines the eigenvalues of seismically isolated bridges free to translate at the end abutments.

The paper concludes that, regardless of the value of the longitudinal isolation period of the deck, the length of the bridge and the number of spans; the first transverse (isolation) period is always longer than the longitudinal isolation period of the deck. This result cannot be captured with the limiting idealization of a beam on continuously distributed springs (beam on Winkler foundation) which yields the opposite result –that the first transverse period is always shorter than the longitudinal isolation period.

Furthermore, when the stiffness of the isolation bearings is relatively small compared to the stiffness of the deck (as in the case of medium size bridges, say $L < 300m$), the isolated deck tends to translate along the transverse direction with a nearly rigid body motion and the transverse isolation period tends to the longitudinal isolation period. On the other hand, when the distributed stiffness of the beam on Winkler foundation is relatively small compared to the stiffness of the deck with length L, the first transverse period of the system is the first flexural period of a free-free end beam, $T_{T1}^{FF} = 8/(9\pi)\sqrt{mL^4/EI}$ –a fundamentally different behavior.

This fundamental difference in the behavior of the two systems has not received the attention it deserves given that occasionally beams isolated on distinct springs with stiffness, K, and spaced at equal distances, d, are invariably treated in the literature as beams on continuously distributed springs with coefficient $k = K/d$ (Ugural and Fenster 1995).

Our study proceeds with the mathematical analysis of the two limiting-case mechanical models: (a) that of a flexural beam supported with continuously distributed springs (beam on Winkler foundation); and (b) that of an isolated beam with isolation bearings at its two ends and at its mid-span. The analytical results derived in this study are confirmed numerically with commercially available software on a four-span and an eight-span isolated deck. The entire modal analysis presented in this paper hinges upon a linear bearing behavior; therefore, it assumes that the isolated system is fully engaged and that the displacements above isolators are large enough so that the second slope of the bilinear idealization of the bearings controls the response. This analysis is conducted within the context of the linear theory of seismic isolation in analogy to the modal analysis presented for the 2-dof isolated structures presented in textbooks (Kelly 1997).

MECHANICAL IDEALIZATION OF ISOLATED BRIDGES

Figure 1 shows the mechanical idealization of a seismically isolated bridge where the longitudinal and transverse motion of the deck is isolated with springs at the center piers and at the abutments. In order to capture the dynamic behavior of the mechanical configuration shown in Figure 1 we examine the mathematical solution of the two limiting cases–those of a beam that is fully isolated in both directions and has either (a) infinite distributed longitudinal and transverse springs along its span (beam on Winkler supports) as shown in Figure 2, or (b) longitudinal and transverse isolation springs at the mid-span and the end abutments as shown in Figure 3.

In this paper we examine the transverse versus the longitudinal eigenperiods of an isolated deck assuming that the isolation bearings are supported on rigid supports in an effort to bring forward the main characteristics of the dynamics of the system. In reality most bridge decks are supported on piers with finite flexibility and this results

in a minor increase of both transverse and longitudinal periods. More specifically, given that most bridge piers have their strong axis along the direction of the deck and their weak axis perpendicular to the direction of the deck, the longitudinal period tends to lengthen slightly more than the transverse period (Buckle et al. 2006); therefore, modifying the results presented in this work which are for rigid piers in both directions. It is worth mentioning that the effect of soil-structure interaction on the lengthening of the isolation periods is marginal (of the order of 1.5% to 2.5%) even for cases with $E_p / E_s = 1000$ (E_p and E_s are Young modulus of piles and soil respectively).

LONGITUDINAL AND TRANSVERSE EIGENVALUES OF A PRISMATIC BEAM WITH CONTINUOUSLY DISTRIBUTED SPRINGS

For a beam on continuously distributed elastic supports with stiffness $k\,[F]/[L]^2$ and distributed mass, $m\,[M]/[L]$; and assuming that the axial rigidity of the beam is large compared to its flexural rigidity EI, its first longitudinal eigenvalue is the isolation frequency along the longitudinal direction i.e.

$$\omega_{L1} = \omega_{IL} = \sqrt{\frac{kL}{mL}} = \sqrt{\frac{k}{m}} \ . \tag{1}$$

The configuration of a beam with distributed elastic support is examined given that in the literature the problem of a long beam supported by individual springs with stiffness K, spaced at equal distance d, is simplified by replacing the individual supports with continuously distributed springs with coefficient $k = K / d$ (Ugural and Fenster 1995).

Under free vibration, the dynamic equilibrium of a beam with flexural rigidity EI along the transverse direction gives (Timoshenko et al. 1974, among others)

$$EI\frac{d^4w(x)}{dx^4}+(k-m\omega^2)w(x)=0. \tag{2}$$

where $w(x)$ is the transverse deflection of the beam along its length.

Case 0: $k-m\omega^2=0$

We examine whether the beam with distributed elastic supports may possess a transverse eigenfrequency equal to the longitudinal eigenfrequency $\omega=\omega_{IT}=\omega_{IL}=\sqrt{k/m}$. In this event, $k=m\omega^2$, and Equation (2) contracts to :

$$EI\frac{d^4w(x)}{dx^4}=0 \tag{3}$$

The solution of Equation (3) is

$$w(x)=Ax^3+Bx^2+Cx+D \tag{4}$$

The boundary conditions of this configuration for vibrations along the transverse direction are zero moments ($d^2w(0)/dx^2=d^2w(L)/dx^2=0$) and zero shear forces ($d^3w(0)/dx^3=d^3w(L)/dx^3=0$) at the end-abutments. Given that the second derivative of Equation (4) is

$$\frac{d^2w(x)}{dx^2}=6Ax+2B, \tag{5}$$

the condition $d^2w(0)/dx^2=0$ yields $B=0$; and upon enforcing the condition $d^2w(L)/dx^2=0$, then $A=0$. The value of $A=0$ also satisfies the boundary conditions for zero shear forces at the end abutments. Accordingly for the case $k=m\omega^2$, the elastic line of the beam on distributed springs is $w(x)=Cx+D$, which is the equation of a straight line; therefore, there is no transverse flexure of the beam.

Consequently, in the event that $\omega_{T1} = \omega = \sqrt{k/m}$, the isolated deck can only experience transverse rigid body motion (translation and rotation) with frequency equal to the longitudinal frequency $\omega_{IL} = \sqrt{k/m}$.

Case 1: $k - m\omega^2 > 0$

For $k - m\omega^2 > 0$ the solution of Eq. (2) is well known to the literature (Timoshenko et al. 1974, Ugural and Fenster 1995 among others),

$$w(x) = e^{\lambda x}(A\cos\lambda x + B\sin\lambda x) + e^{-\lambda x}(C\cos\lambda x + D\sin\lambda x), \quad (6)$$

where

$$\lambda^4 = \frac{k - m\omega^2}{4EI} > 0. \quad (7)$$

With the aforementioned boundary conditions for flexure along the transverse direction $d^2w(0)/dx^2 = d^3w(0)/dx^3 = d^2w(L)/dx^2 = d^3w(L)/dx^3 = 0$, the eigenvalues of the problem are obtained from the solution of the homogeneous system

$$\begin{bmatrix} 0 & 1 & 0 & -1 \\ -1 & 1 & 1 & 1 \\ -e^{\lambda L}\sin\lambda L & e^{\lambda L}\cos\lambda L & e^{-\lambda L}\sin\lambda L & -e^{-\lambda L}\cos\lambda L \\ -e^{\lambda L}(\sin\lambda L + \cos\lambda L) & e^{\lambda L}(\cos\lambda L - \sin\lambda L) & e^{-\lambda L}(\cos\lambda L - \sin\lambda L) & e^{-\lambda L}(\cos\lambda L + \sin\lambda L) \end{bmatrix} \begin{Bmatrix} A \\ B \\ C \\ D \end{Bmatrix} = \begin{Bmatrix} 0 \\ 0 \\ 0 \\ 0 \end{Bmatrix}$$

(8)

The solution of the associated characteristic equation is given by:

$$\cosh(2\lambda L) = 2 - \cos(2\lambda L) \quad (9)$$

Equation (9) can be satisfied only when $\lambda L = 0$ (see graphs on Figure 4) which implies that $\lambda = 0$. For $\lambda = 0$ Equation (7) gives that $k - m\omega^2 = 0$ –a finding that contradicts the initial assumption of this case, that $k - m\omega^2 > 0$. The above analysis shows that when the frequency is kept low enough so that $k - m\omega^2 > 0$, then this low

frequency range does not contain any eigenvalues of the structure along the transverse direction. Accordingly, the eigenvalues of the system belong in the range $k - m\omega^2 < 0$.

Case 2: $k - m\omega^2 < 0$

For $k - m\omega^2 < 0$ the solution of Equation (2) is also well known in the literature (Timoshenko et al. 1974, Clough and Penzien 1993),

$$w(x) = A\cos\lambda x + B\sin\lambda x + C\cosh\lambda x + D\sinh\lambda x \qquad (10)$$

where now,

$$\lambda^4 = \frac{m\omega^2 - k}{EI} > 0 \qquad (11)$$

By applying the zero moment and zero shear boundary conditions the eigenvalues of the problem are obtained from the solution of the homogeneous system,

$$\begin{bmatrix} 0 & -1 & 0 & 1 \\ -1 & 0 & 1 & 0 \\ -\sin\lambda L & -\cos\lambda L & \sinh\lambda L & \cosh\lambda L \\ -\cos\lambda L & \sin\lambda L & \cosh\lambda L & \sinh\lambda L \end{bmatrix} \begin{Bmatrix} A \\ B \\ C \\ D \end{Bmatrix} = \begin{Bmatrix} 0 \\ 0 \\ 0 \\ 0 \end{Bmatrix}. \qquad (12)$$

The characteristic equation of the system reduces to

$$\cosh\lambda L\cos\lambda L = 1 \qquad (13)$$

and the solutions of Equation (13) lead to the eigenfrequencies

$$\omega_{Tn} = \sqrt{\frac{k}{m} + (n + \frac{1}{2})^4 \pi^4 \frac{EI}{mL^4}}, \quad n \in \{1,2,...\} \qquad (14)$$

Equation (14) shows that the lowest transverse eigenfrequency ($n = 1$) of the isolated deck is $\omega_{T1} = \sqrt{k/m + (3\pi/2)^4 EI/mL^4}$; therefore, it will always be larger than the first longitudinal isolation frequency $\omega_{L1} = \sqrt{k/m}$ (rigid body motion along the longitudinal direction). Consequently, the limiting case model which idealizes the isolated deck on distinct isolation bearings with a flexural beam with continuously distributed springs yields that, no matter how long the bridge is, the first transverse

isolated period that involves flexure of the deck is always smaller (stiffer configuration) than the longitudinal isolation period.

At this point it is interesting to note that the eigenfrequencies of a beam on Winkler foundation with free-free ends are higher (stiffer configuration) than the eigenfrequencies when both ends are pinned. This result is consistent with the result that a "flying" oscillating beam (free-free end) has higher eigenfrequencies (those of the fixed-fixed end beam) than the eigenfrequencies of a pinned-pinned end beam (Timoshenko et al. 1974). Table 1 summarizes the characteristic equations and the resulting transverse eigenvalues for a free-free end and a pinned-pinned end beam on Winkler foundation.

LONGITUDINAL AND TRANSVERSE EIGENVALUES OF A BEAM WITH A LONGITUDINAL AND TRANSVERSE SPRING AT ITS MID-SPAN AND ITS SUPPORTS

We now proceed with the eigenvalue analysis of the other limiting mechanical idealization–that of a beam where its longitudinal and transverse motion is isolated with springs at its three supports (see Figure 5).

Transverse Periods

Given the symmetry of the problem we can analyze half of the beam with $l = L/2$ as shown in Figure 5. Note that this model yields only the symmetric modes.

The solution of the vibration of a beam with flexural rigidity, EI and distributed mass, m is (Timoshenko et al. 1974, Clough and Penzien 1993, Chopra 2001 among others),

$$w(x) = A\sin\lambda x + B\cos\lambda x + C\sinh\lambda x + D\cosh\lambda x \qquad (15)$$

where now

$$\lambda = \sqrt[4]{\frac{m\omega^2}{EI}} > 0 \qquad (16)$$

The boundary conditions of this configuration for vibrations along the transverse directions at the left end-support are zero bending moment ($d^2w(0)/dx^2 = 0$), and shear force equal the spring reaction, $-EI\, d^3w(0)/dx^3 = K_A w(0)$, while at the right end ($x = l = L/2$) the slope is zero $dw(l)/dx = 0$ and the shear force equals half the spring reaction $EI\, d^3w(l)/dx^3 = (K_M/2)\, w(l)$. In the above expressions K_A and K_M are the stiffnesses of the bearing(s) at the abutment and at the central pier (mid-span) respectively.

With the abovementioned boundary conditions the eigenvalues of the system for vibrations along the transverse direction are obtained from the solution of the homogeneous system.

$$\begin{bmatrix} 0 & -\lambda^2 & 0 & \lambda^2 \\ -\lambda^3 & \frac{K_A}{EI} & \lambda^3 & \frac{K_A}{EI} \\ \lambda\cos\lambda l & -\lambda\sin\lambda l & \lambda\cosh\lambda l & \lambda\sinh\lambda l \\ -\lambda^3\cos\lambda l - \frac{K_M}{2EI}\sin\lambda l & \lambda^3\sin\lambda l - \frac{K_M}{2EI}\cos\lambda l & \lambda^3\cosh\lambda l - \frac{K_M}{2EI}\sinh\lambda l & \lambda^3\sinh\lambda l - \frac{K_M}{2EI}\cosh\lambda l \end{bmatrix} \begin{Bmatrix} A \\ B \\ C \\ D \end{Bmatrix} = \begin{Bmatrix} 0 \\ 0 \\ 0 \\ 0 \end{Bmatrix}$$

The associated characteristic equation is

$$\begin{aligned} &2\lambda^3\cosh\lambda l\cos\lambda l[(-\lambda^6 - \frac{K_A}{EI}\frac{K_M}{2EI})\tanh\lambda l + (-\lambda^6 + \frac{K_A}{EI}\frac{K_M}{2EI})\tan\lambda l + \\ &2\lambda^3\frac{K_A}{EI} + (1 + \frac{1}{\cosh\lambda l\cos\lambda l})\lambda^3\frac{K_M}{2EI}] = 0 \end{aligned} \qquad (17)$$

Equation (17) is satisfied either when $\cos\lambda l = 0$, or when the quantity in brackets is equal to zero. The condition $\cos\lambda l = 0$ corresponds to $\lambda l = (2n+1)(\pi/2)$, which gives the eigenvalues of the simply supported beam (without the spring at the mid-span). The first transverse period, T_{T1}^{SS}, of the simply supported beam with length L is

$$T_{T1}^{SS} = \frac{2}{\pi}\sqrt{\frac{mL^4}{EI}} \tag{18}$$

while the second modal period, $T_{T2}^{SS} = T_{T1}^{SS}/4$. By setting the quantity in brackets in Equation (17) equal to zero, one obtains

$$\tanh \lambda l = \frac{1}{\xi_A \xi_M + 2(\lambda l)^6}\{[\xi_A \xi_M - 2(\lambda l)^6]\tan \lambda l + 4(\lambda l)^3 \xi_A + (1 + \frac{1}{\cosh \lambda l \cos \lambda l})(\lambda l)^3 \xi_M\} \tag{19}$$

where $\xi_A = K_A L^3/(8EI)$, $\xi_M = K_M L^3/(8EI)$ are dimensionless parameters which express the relative contribution of the stiffness of the isolation bearings at the abutment and the mid-span, to the transverse flexural rigidity of the deck respectively. We first examine the limiting expressions of Equation (19) as ξ_A and ξ_M tend to various limiting values. When $\xi_A \to \infty$ (very stiff springs at the end-abutments), Equation (19) reduces to Equation (16) in the paper by Makris et al. (2010)

$$\tanh \lambda l = \tan \lambda l + \frac{4(\lambda l)^3}{\xi_M}, \tag{20}$$

which describes the transverse behavior of a simply supportedbeam with an elastic spring in the mid-span. According to Makris et al. (2010) as $\xi_M \to \infty$ (very stiff spring at the mid-span or very soft deck) Equation (20) reduces to $\tanh \lambda l = \tan \lambda l$ which is the characteristic equation of a beam with length $l = L/2$ and with one end simply supported while the other end is fixed. In this case the first root is $\lambda l = (1+1/4)\pi = 5\pi/4$ and the first modal period of this configuration is

$$T_{T1}^{SF(L/2)} = \frac{8}{25\pi}\sqrt{\frac{mL^4}{EI}} = \frac{4}{25}T_{T1}^{SS}. \tag{21}$$

On the other hand, when $\xi_M \to 0$ and $\xi_A \to \infty$, Equation (19) yields the solution that corresponds to a simply supported beam with length $L = 2l$, i.e. $\lambda l = \pi/2$. Now when

both spring stiffnesses are zero, $\xi_A = \xi_M = 0$,(vibrating beam with free ends), Equation (19) contracts to

$$\tanh \lambda l = -\tan \lambda l . \tag{22}$$

Equation (22) offers the odd roots of Equation (13) which is the characteristic equation of a beam with fixed-fixed ends and length $L = 2l$ (see graphs in Figure 4). The reason that Equation (22) offers only the odd roots is that the semi-beam shown in Figure 5 can capture only the symmetric mode shapes. Equation (22) does not capture the rigid body motion but only frequencies associated with flexure. The first root of Equation (22) is $\lambda l = 3\pi/4 = 2.356$ (see Figure 4) and the corresponding modal period is

$$T_{T1}^{\ FF} = \frac{8}{9\pi}\sqrt{\frac{mL^4}{EI}} = \frac{4}{9}T_{T1}^{\ SS} . \tag{23}$$

However, when one approaches the zero-stiffness limit by letting the values of the spring stiffnesses tend gradually to zero ($\xi_A \to 0$, $\xi_M \to 0$) with Equation (19), an early root of the original Equation (19) appears which corresponds to the gradual degeneration of the flexural mode to a rigid body mode (see Figure 6). Figure 6 plots the left-hand side $= \tanh \lambda l$ and the right-hand side of Equation (19) for a small value of $\xi_M = 0.01$. As stated before, as ξ_M tends to zero the right-hand side of Equation (20) exhibits a small hump at the early values of λl which crosses the function $\tanh \lambda l$. The value of $\lambda l = \lambda L/2$ where this early crossing happens corresponds to the first mode of the system which, while containing some mild flexure of the beam, is essentially a rigid body mode. The next solution of the transcendental Equation (19) is $\lambda l = \lambda L/2 = 3\pi/4 = 2.356$ (see Figure 6) and corresponds to the first flexural mode of a free-free end beam as predicted by Equation (22). As ξ_M tends continuously to zero, the early hump that produces the

solution corresponding to the rigid body mode is further squeezed in the vicinity of zero bringing the corresponding mode closer and closer to a fully rigid body mode.

a) Spherical-Sliding Bearings

We consider now the case where the two-span bridge of Figure 5 is supported at each of the three supports (end-abutments and mid-span) on identical spherical sliding bearings with radius of curvature R, both in longitudinal and transverse direction. Given that the two-span beam is a continuous beam, the vertical reaction at the midspan bearing is $N_M = 5/8\, mgL$, while the vertical reaction at each of the end-bearings is $N_A = 3/16\, mgL$. Accordingly, the lateral stiffness of the center spherical sliding bearing and of the bearing above the abutment is, $K_M = N_M / R = 5/8\, mgL/R$ and $K_A = N_A / R = 3/16\, mgL/R$ respectively. The relation between the two dimensionless stiffnesses is

$$\frac{\xi_A}{\xi_M} = \frac{\dfrac{K_A L^3}{8EI}}{\dfrac{K_M L^3}{8EI}} = \frac{K_A}{K_M} = \frac{\dfrac{3mgL}{16R}}{\dfrac{5mgL}{8R}} = \frac{3}{10} \Rightarrow \quad \xi_A = 0.3\xi_M \qquad (24)$$

b) Elastomeric Bearings

When the two-span deck of Figure 3 is supported at each of the three supports (end abutments and mid-span), both in longitudinal and transverse direction on identical elastomeric bearings with lateral stiffness $K = K_A = K_M$, the relation between the dimensionless bearing stiffnesses becomes,

$$\frac{\xi_A}{\xi_M} = \frac{K_A}{K_M} = 1 \Rightarrow \quad \xi_A = \xi_M \qquad (25)$$

Thus, for a given value of ξ_M, Equation (19) yields different results for the two types of isolation bearings.

The solution of the transcendental Equation given by (19) is obtained for various values of $\xi_{A,}\,\xi_M$ either numerically with a Newton-Raphson method or graphically with the Creskoff diagram shown in Figure 7. Figures 6 and 7 show that, for finite values of, $\xi_A = K_A L^3/8EI$, $\xi_M = K_M L^3/8EI$, the transcendental Equation (19) has real and positive solutions, say $S(\xi_A,\xi_M) = \lambda(\xi_A,\xi_M)l$ with $l = L/2$ and $\lambda(\xi_A,\xi_M) = \sqrt[4]{m\omega^2(\xi_A,\xi_M)/EI} > 0$.

Accordingly,

$$S(\xi_A,\xi_M) = \frac{L}{2}\sqrt[4]{\frac{m\omega_T{}^2(\xi_A,\xi_M)}{EI}} \tag{26}$$

or

$$\omega_T(\xi_A,\xi_M) = 4S^2(\xi_A,\xi_M)\sqrt{\frac{EI}{mL^4}}\,. \tag{27}$$

Equation (26) with the help of Equation (18) gives

$$\frac{T_T}{T_{T1}{}^{SS}} = \frac{\pi^2}{4}\frac{1}{S^2(\xi_A,\xi_M)} \tag{28}$$

in which, T_T , is the transverse period of the two-span isolated beam. Figure 8 plots the expression given by Equation (28) after finding the roots of Equation (19), $S(\xi_A,\xi_M) = \lambda(\xi_A,\xi_M)l$, for the range of ξ_A and ξ_M that is of interest.

Figure 8 plots the eigenvalues of the two-span bridge in logarithmic scale. In addition to the solid dark lines which plot the results of Equation (28), Figure 8 presents with isolated points (circles and squares) the solution that one obtains for the same problem by using the commercially available software SAP (Computers and Structures 2006). Note that the software captures with great accuracy the first and second transverse periods of the bridge for both configurations with either spherical sliding bearings (FPS) or elastomeric bearings (EB). In the SAP analysis the bearings

are merely modeled with linear elastic springs. For spherical sliding bearings the corresponding spring stiffness is $K = N / R$, where N is the vertical load on the bearing and R is the radius of curvature of the bearing. When elastomeric bearings are used the stiffness of the idealized springs is the second slope of the force-displacement loop of the elastomeric bearing—the slope that defines the isolation period.

The chained lines appearing in Figure 8 show the transverse eigenperiod that one computes by using the solution of the beam on a Winkler foundation $T_{T1} = 2\pi / \sqrt{k/m + (3\pi/2)^4 EI/(mL^4)}$ in which $k = (mgL/R)/L = mg/R$ for the spherical sliding bearings and $k = 3K_M / L$ for the elastomeric bearings. What is most interesting about this idealization is that, as the value of the distributed stiffness k tends to zero, the solution of the beam on Winkler foundation given by (13) and (14) tends to the first flexural mode of a free-free end beam $T_{T1}^{FF} = 8/9\pi\sqrt{mL^4/EI}$ – not to the translational rigid-body mode with period $T_{T1} = 2\pi\sqrt{R/g}$ for spherical sliding bearings or $T_{T1} = 2\pi\sqrt{mL/3K_M}$ for elastomeric bearings which are the straight dashed lines in Figure 8 (bottom). It is worth noting that the solutions for the transverse periods of an isolated deck on distinct bearings in the bottom plot of Figure 8 appear to "avoid" the solutions for the transverse periods of a beam on Winkler foundation that has the same longitudinal isolation period as the deck on distinct isolation bearings. Similar trends are observed in the eigenvalue analysis of decks with a larger number of spans.

Longitudinal Periods

a) Spherical-Sliding Bearings

When the two-span bridge of Figure 5 is supported at each of the three supports (end-abutments and mid-span) on identical spherical sliding bearings with radius of curvature R, the longitudinal period is

$$T_L^{FPS} = 2\pi\sqrt{\frac{R}{g}}. \tag{29}$$

Recalling that the two-span beam is a continuous beam, the vertical reaction at the center bearing is $N_M = 5/8\, mgL$, while the vertical reaction at each of the end-bearings is $N_A = 3/16\, mgL$. Accordingly, the lateral stiffness of the center spherical sliding bearing is, $K_M = N_M / R = 5/8\, mgL/R$ and the dimensionless stiffness of the center bearing is

$$\xi_M = \frac{K_M L^3}{8EI} = \frac{5}{64}\frac{mgL^4}{REI} \tag{30}$$

Substitution in (30) of the ratio g/R from Equation (29) gives,

$$\frac{T_L^{FPS}}{T_{T1}^{SS}} = \sqrt{\frac{5}{4}}\frac{\pi^2}{4}\frac{1}{\sqrt{\xi_M}} \tag{31}$$

Figure 8 also plots with thin dashed line the expression given by Equation (31) together with the solution given by Equation (28) in which $\xi_A = 0.3\xi_M$. Note that the line obtained from Equation (28) is always above the line given by Equation (31). This result, which becomes more visible in the bottom plot of Figure 8 (vertical axis in logarithmic scale), shows that the transverse isolation period is always longer than the longitudinal isolation period, $T_L^{FPS} = 2\pi\sqrt{R/g}$, regardless of the length of the bridge. This remarkable result also holds for the case where the deck is isolated on elastomeric bearings.

b) Elastomeric Bearings

In the case that the two-span deck of Figure 5 is supported at each of the three supports (end abutments and mid-span) on identical elastomeric bearings with lateral stiffness $K_M = K_A$, the longitudinal period of the bridge is

$$T_L^{EB} = 2\pi\sqrt{\frac{mL}{3K_M}} \tag{32}$$

The dimensionless stiffness of the bearing, $\xi_M = K_M L^3 / 8EI$, gives

$$K_M = \frac{8\xi_M EI}{L^3} \tag{33}$$

Substitution of Equation (33) in (32) gives,

$$T_L^{EB} = \frac{1}{\sqrt{6}}\frac{1}{\sqrt{\xi_M}}\pi\sqrt{\frac{mL^4}{EI}} \tag{34}$$

From Equation (18) the first transverse period of the simply supported beam with length L is $T_{T1}^{SS} = \frac{2}{\pi}\sqrt{mL^4/EI}$, and therefore Equation (34) gives

$$\frac{T_L^{EB}}{T_{T1}^{SS}} = \sqrt{\frac{2}{3}}\frac{\pi^2}{4}\frac{1}{\sqrt{\xi_M}} \tag{35}$$

Figure 8 also plots with a heavy dashed line the expressions given by Equation (35) next to the line given by Equation (28) where now $\xi_A = \xi_M$. Note that the transverse isolation period is always longer than the longitudinal isolation period, given by Equation (35); however, it is evident that the solution that corresponds to the

spherical sliding bearings (FPS) case is always above (longer normalized transverse periods) the solution that corresponds to the elastomeric bearings (EB) case.

THE TRANSVERSE EIGENVALUES OF MULTI-SPAN ISOLATED BRIDGES

Our investigation proceeds with the analysis of a 4-span and an 8-span isolated deck. Similarly to the mechanical idealization shown in Figure 1, the 4-span and 8-span isolated decks are fully isolated along the longitudinal and transverse direction. A series of eigenvalue analyses have been conducted using the software SAP (Computer and Structures 2006) for bridge decks with $E_c = 25000MPa$, $I = 100m^4$, $m = 50Mg/m$, different values of length, L , and isolation periods along the longitudinal direction $T_L \approx 3.0s$ and $T_L \approx 2.0s$. Both spherical sliding ($R = 2.2m$ for $T_L \approx 3.0s$ and $R = 1.0m$ for $T_L \approx 2.0s$) and elastomeric bearings have been considered. Figure 9 (top) plots the first transverse period, T_{T1} , of the 4-span isolated deck normalized to the longitudinal isolation period, T_L , as a function of the length of the deck. For a 4-span deck the longitudinal period is given either by Equation (29) in which R is the radius of curvature of any of the identical spherical sliding bearings, or by

$$T_L = T_L^{EB} = 2\pi\sqrt{\frac{mL}{5K}} \tag{36}$$

where K is the lateral stiffness of any of the identical elastomeric bearings at each support. Regardless of the value of the isolation period, T_L , and whether the deck is isolated on spherical sliding bearings or elastomeric bearings, the ratio T_{T1}/T_L is above unity in all cases.

Figure 9 (bottom) shows that the same pattern is observed in the case of an 8-span deck. In the event that the 8-span deck is isolated at each of its nine (9) supports with elastomeric bearings having stiffness, K , the longitudinal period is given by

$T_L = T_L^{EB} = 2\pi\sqrt{mL/9k}$, while T_L^{FPS} is given by Equation (29).

We are now interested in examining whether the four (4) distinct response curves shown at the top and bottom of Figure 9 are related to each other; or each one of them contains independent information. Whereas the ratio T_{T1}/T_L is dimensionless, it is not the appropriate dimensionless product to extract the physics of the problem. With simple arguments from dimensional analysis (Barenblatt 1996, Langhaar 1951) one can show that in order to uncover any existence of self-similar response, the transverse period of the deck needs to be normalized to a time scale that reflects the flexural rigidity of the deck; whereas, the horizontal axis shall reflect the normalized lateral stiffness of the bearings, K , at a single support to the flexural rigidity of the deck (EI/L^3) (Makris et al. 2010). Figure 10 (top) presents the same information as Figure 9 (top) in terms of dimensionless products $\Pi_T = T_{T1}/T_{T1}^{SS}$ and $\Pi_K = \xi_M = K_M L^3/8EI$ where T_{T1}^{SS} is given by Equation (18).

Interestingly, the four distinct response curves, appearing in Figure 10 (top) are very close to each other and eventually form a single master curve for values of $\xi_M > 20$. This single master curve shown in Figure 10 (top) is independent of the longitudinal isolation period of the deck. At the low range of ξ_M ($\xi_M < 20$) the first normalized transverse periods of the deck when supported on spherical sliding bearings are slightly higher than the corresponding transverse periods of a deck supported on elastomeric bearings following the same trend that was computed analytically for the two-span deck shown in Figure 8. What however is most important to note is that the normalized transverse periods, T_{T1}^{FPS}/T_{T1}^{SS} and T_{T1}^{EB}/T_{T1}^{SS} are, for any given value

of ξ_M , above the normalized corresponding longitudinal isolation periods, T_L^{FPS}/T_{T1}^{SS} and T_L^{EB}/T_{T1}^{SS}, respectively. The same remarkable self-similar response emerges in Figure 10 (bottom) for the eight-span deck.

Now, one shall notice that the self-similar response curves for the 4-span deck on Figure 10 (top) and the 8-span deck on Figure 10 (bottom), have also similar shapes. Nevertheless, the horizontal axis in Figure 10 is $\Pi_K = \xi_M = K_M L^3/8EI$, which is the normalized lateral stiffness of the bearings at a single support to the flexural rigidity of the deck. For any given value of $\xi_M = K_M L^3/8EI$, the eight-span deck enjoys the restoring transverse force from the bearings at nine (9) supports; whereas, the four-span deck enjoys the transverse restoring force from the bearings at only five (5) supports.

We are now interested in assessing the transverse contribution of the bearings at all the supports of a multi-span bridge. The challenge with the free-free end configuration is that for small values of ξ_M the deformed shape of the deck is a nearly straight line parallel to the original position (rigid body motion); therefore, all bearings are deforming by almost the same amount. On the other hand, for large values of ξ_M the deformed shape of the deck resembles a half sine wave; therefore, the bearings supporting the center span are deforming more than the bearings supporting the end-spans. In a related publication, Makris et al. (2010), have shown that the transverse participation of all bearings in an n-span bridge is proportional to $(n/2)\xi_M$. Figure 11 plots the same information presented in Figure 10 (top and bottom) together with the results of Equation (19) (two-span deck) where now the horizontal axis is $(n/2)\xi_M = nK_M L^3/(16EI)$ where n is the number of spans. Interestingly, all curves of the normalized transverse periods (two-span, four-span and eight-span bridges) collapse to a self-similar solution, indicating that the first

transverse eigenperiod of any multi-span isolated deck is given by a single master curve.

It is worth noting in Figure 11 that beyond the value $(n/2)\xi_M \approx 50$ the transverse period of the 2-span deck departs from the single master curve. This is because beyond $\xi_M = 50\,(n=2)$ the spring at the mid-span is stiff enough so that the mode shape of the bridge departs appreciably from the half-sine and tends to the mode shape of the beam with length $l = L/2$ and with one end simply supported and the other end fixed (Makris et al. 2010).

Figure 11 plots the computed first transverse periods of the two-span, the four-span, and the eight-span isolated deck in a logarithmic scale as a function of $(n/2)\xi_M$. The self-similar response from all configurations forms a single master curve which is plotted with a heavy gray straight line. Regression analysis from all the points appearing in Figure 11 resulted in the expression

$$\ln\left(\frac{T_{T1}^{MS}}{T_{T1}^{SS}}\right) = -0.475\ln\left(\frac{n}{2}\xi_M\right) + 0.775. \qquad (37)$$

The expression given by Equation (37) can be used with confidence to estimate the first transverse eigenperiod of any multi-span bridge with its deck fully isolated at all its supports. Typical lengths of spans in prestressed isolated bridges are between 35m and 45m while a span of 60m is on the high end. For all practical values of the section and material properties of a deck that is physically realizable ($I \approx 100m^4$, $E \approx 25MPa$), the values of the dimensionless ratio $(n/2)\xi_M$ are below 50, showing that the master curve given by equation (37) can be used with confidence. To this end the chained lines appearing in Figure 8 show the transverse eigenperiods that one computes by using the solution of the beam on a Winkler foundation, $T_{T1} = 2\pi/\sqrt{k/m + (3\pi/2)^4 EI/(mL^4)}$ in which $k = mg/R$ for the spherical sliding

bearings and $k = (n+1)K_M / L$ for the elastomeric bearings ($n = 2, 4, 8 =$ number of spans). What is most interesting about the beam on Winkler foundation is that as the value of the distributed stiffness, k, tends to zero the solution for the eigenvalues given by (13) and (14) tends to the first flexural mode of a free-free end beam $T_{T1}^{FF} = 8/9\pi\sqrt{mL^4/EI}$ –not to the translational rigid-body mode with period $T_{T1} = \sqrt{R/g}$ for spherical sliding bearings or $T_{T1} = \sqrt{mL/((n+1)K_M)}$ for elastomeric bearings.

CONCLUSIONS

This paper examines the eigenvalues of multi-span long seismically isolated bridges where the deck is fully isolated along the longitudinal and transverse direction, therefore enjoys concentrated restoring forces from the isolation bearings above the piers and the abutments. This study first investigates mathematically the eigenvalue problem of a two-span isolated deck and subsequently examines numerically a 4-span and an 8-span isolated deck. The study concludes that regardless of the value of the isolation period in the longitudinal direction, the length of the bridge and the number of spans, the first transverse isolation period is always longer than the longitudinal isolation period of the deck. This result cannot be captured with the limiting idealization of a beam on continuously distributed springs (beam on Winkler foundation) which yields the opposite result–that the lower transverse period is always shorter than the longitudinal period.

More specifically, when the stiffness of the isolation bearings is relatively small compared to the stiffness of the deck, the first transverse period of the isolated deck tends to the longitudinal period from above (the deck tends to translate along the transverse direction with a rigid-body motion). On the other hand, when the

distributed stiffness of the beam on Winkler foundation is relatively small compared to the stiffness of the deck, the first transverse period of the system is the first flexural period of a free-free end beam–a fundamentally different behavior. This fundamental difference shows that when the distributed stiffness of the beam on Winkler foundation tends to zero the beam tends to a flexural mode–not a rigid body mode (see also Table 1 of this paper) as the deck on distinct isolation bearings does.

Finally, using arguments from dimensional analysis the paper shows that the normalized transverse eigenperiods of any finite-span isolated deck are self-similar solutions that are independent of the longitudinal isolation period of the deck or whether the deck is supported on elastomeric or spherical sliding bearings. In a logarithmic plot this self-similar behavior collapses to a single straight line which offers the first transverse isolation period on any finite-span isolated deck.

ACKNOWLEDGEMENTS

Partial financial support has been provided by the EU research project "DARE" ("Soil-Foundation-Structure Systems Beyond Conventional Seismic Failure Thresholds: Application to New or Existing Structure and Monuments"), which is – Advanced Grant, under contract number ERC-2---9-AdG228254-DARE to Prof. G. Gazetas.

REFERENCES

1. Barenblatt, G., I. *Scaling, self-similarity, and intermediate asymptotics.* Cambridge Texts in Applied Mathematics, Cambridge University Press, 1996.

2. Buckle, I., Constantinou, M., Dicleli, M., Ghasemi, H. “Seismic Isolation of Highway Bridges.”, *MCEER-06-SP07*, State University of New York at Buffalo, 2006.
3. Chopra, A., K. *Dynamics of Structures: Theory and Applications to Earthquake Engineering.* 2nd Edition, Prentice Hall, New Jersey, 2001.
4. Clough, R.W., Penzien, J. *Dynamics of Structures.* 2nd edition, McGraw-Hill, New York, 1993.
5. Computers and Structures. *SAP 2000 Documentation.* University of California, Berkeley, 2006.
6. FHWA. *Seismic Retrofitting manual for Highway Bridges*. U.S. Department of Transportation: U.S.A., 1995.
7. Kelly, J., M. *Earthquake-Resistant design with rubber.* Second Edition, Springer-Verlag, London, 1997.
8. Langhaar, H., L. *Dimensional Analysis and Theory of Models.* Wiley, New York, 1951.
9. Makris, N., Kampas, G., Angelopoulou, D. “The Eigenvalues of Isolated Bridges with Transverse Restraints at the End Abutments.”, *Earthquake Engineering and Structural Dynamics* 2010, 39(8), 869-886.
10. Skinner, R.I., Robinson, W.,H., McVerry, G., H. *An Introduction to Seismic Isolation*. Wiley, New York, 1993.
11. Timoshenko, S., P., Young, D., H., Weaver, W., JR. *Vibration Problems in Engineering* (4^{th} Edition). Wiley, New York, 1974.
12. Ugural, A., C., Fenster, S., K. *Advanced Strength and Applied Elasticity* (3^{rd} Edition). Prentice-Hall, New Jersey, 1995.

Table 1.Eigenfrequencies of a beam on Winkler foundation with finite length L , Left: Free ends, Right:Pinned Ends.

Configuration Plan View	*Free ends*	*Pinned Ends*
Governing Equation:	$EI\frac{d^4w(x)}{dx^4}+(k-m\omega^2)w(x)=0$	
Case 0 $k-m\omega^2=0$	$\lambda=0$ $\omega_{T1}=\sqrt{k/m}$ Rigid body motion	$\lambda=0$ No transverse eigenvalues
Case 1 $k-m\omega^2>0$	$\lambda^4=\frac{k-m\omega^2}{4EI}$ $\cosh(2\lambda L)=2-\cos(2\lambda L)$ No transverse eigenvalues	$\lambda^4=\frac{k-m\omega^2}{4EI}$ $\cos(2\lambda L)=\cosh(2\lambda L)$ No transverse eigenvalues
Case 2 $k-m\omega^2<0$	$\lambda^4=\frac{m\omega^2-k}{EI}$ $\cosh\lambda L\cos\lambda L=1$ $\omega_{Tn}=\sqrt{\frac{k}{m}+(n+\frac{1}{2})^4\pi^4\frac{EI}{mL^4}}, n\in\{1,2,...\}$	$\lambda^4=\frac{m\omega^2-k}{EI}$ $\sinh\lambda L\sin\lambda L=0$ $\omega_{Tn}=\sqrt{\frac{k}{m}+n^4\pi^4\frac{EI}{mL^4}}, n\in\{1,2,...\}$

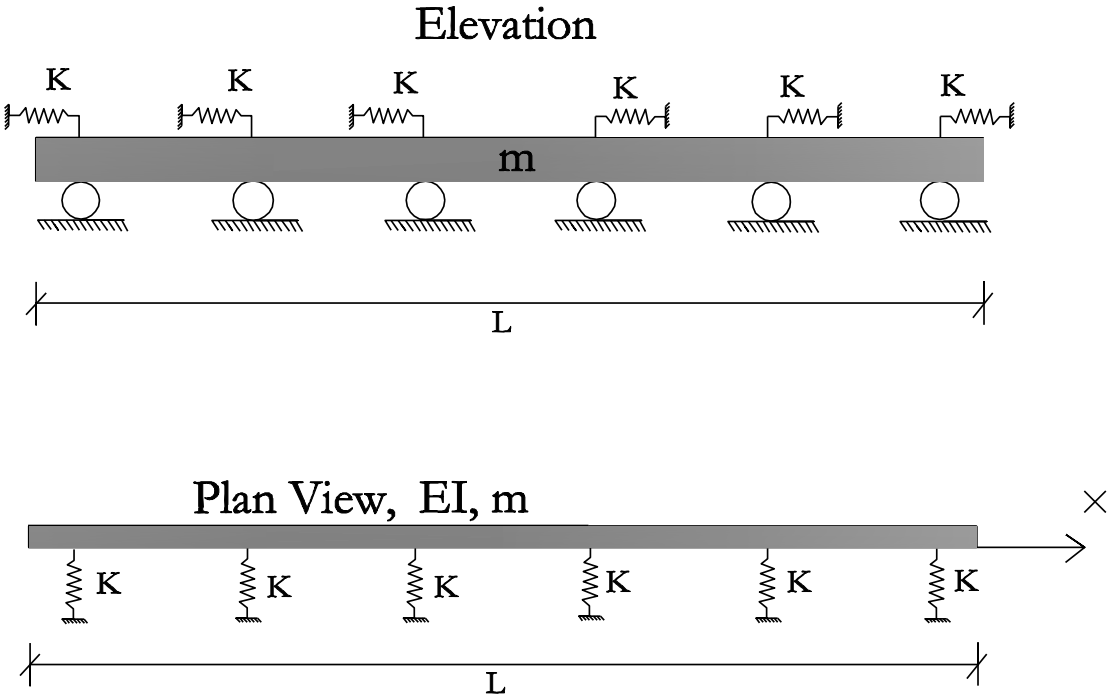

Fig. 1. Mechanical idealization of an isolated deck which is fully isolated along both longitudinal and transverse direction.

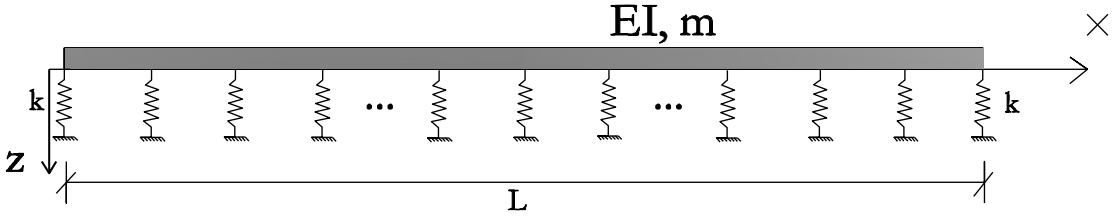

Fig. 2. Plan view of a beam with continuous distributed springs along its length (Winkler foundation).

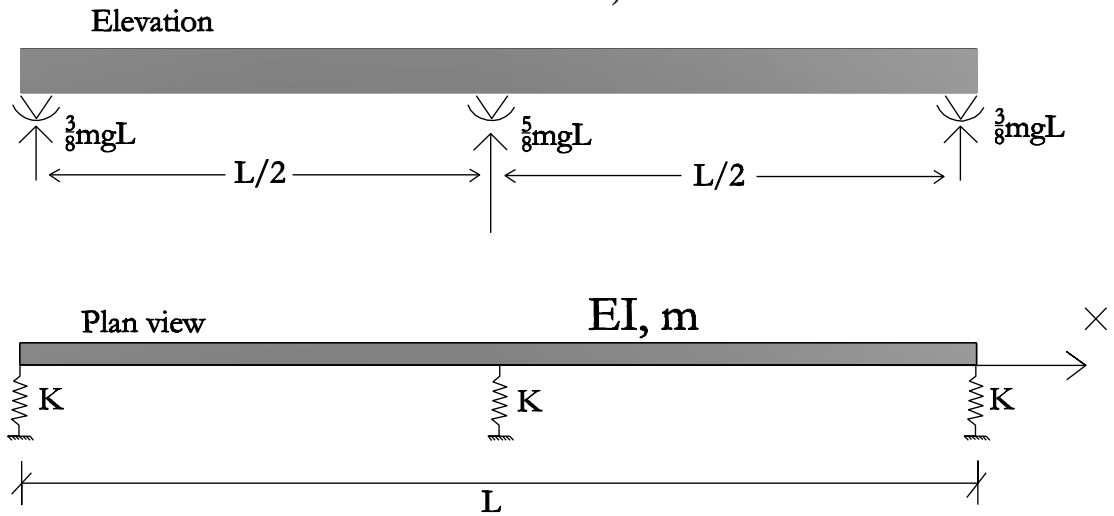

Fig. 3. Elevation (top)and plan view (bottom) of a two-span beam that is fully isolated along the longitudinal and transverse direction.

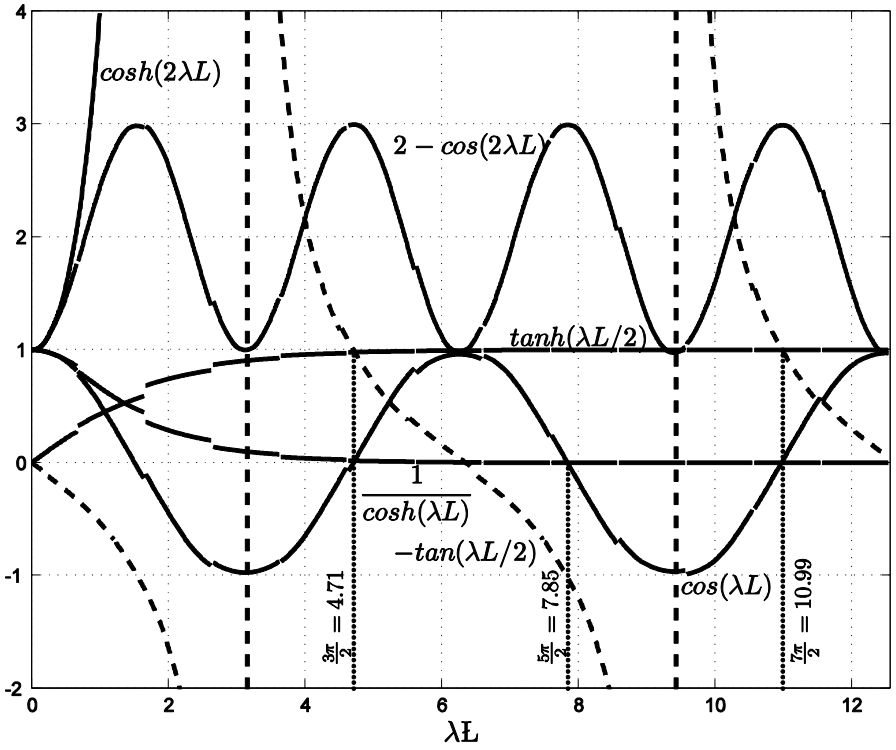

Fig. 4. Graphical solutions of various characteristic equations pertinent in this study.

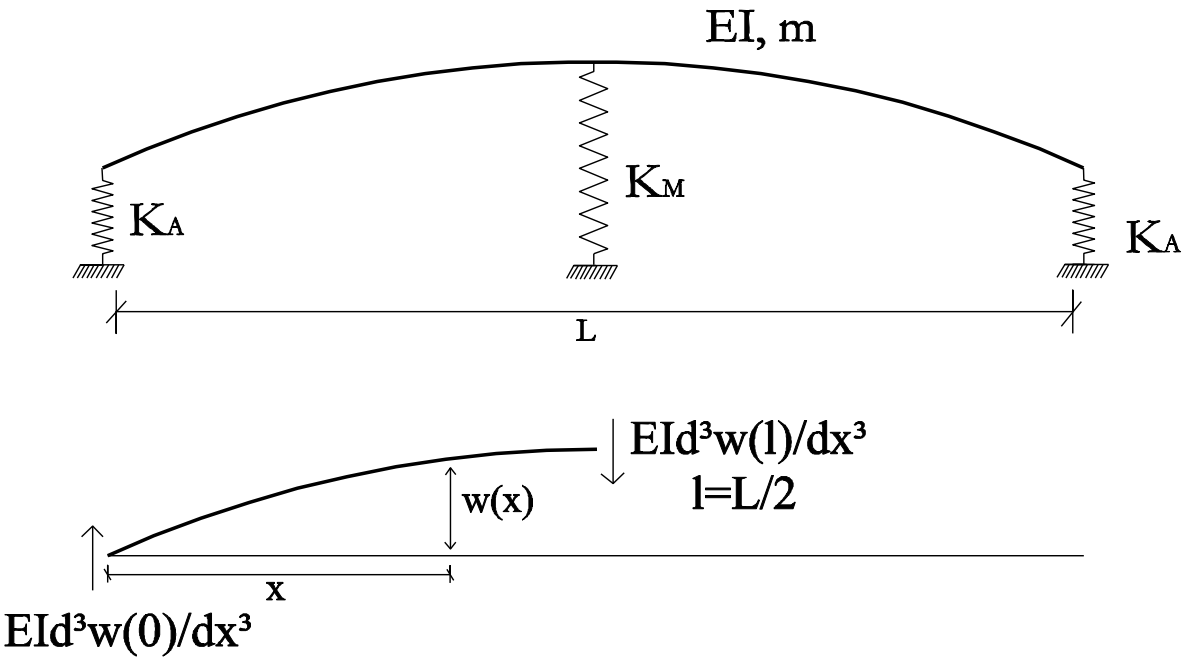

Fig. 5. First transverse mode shape of a two-span isolated deck and free body diagram of its left-half.

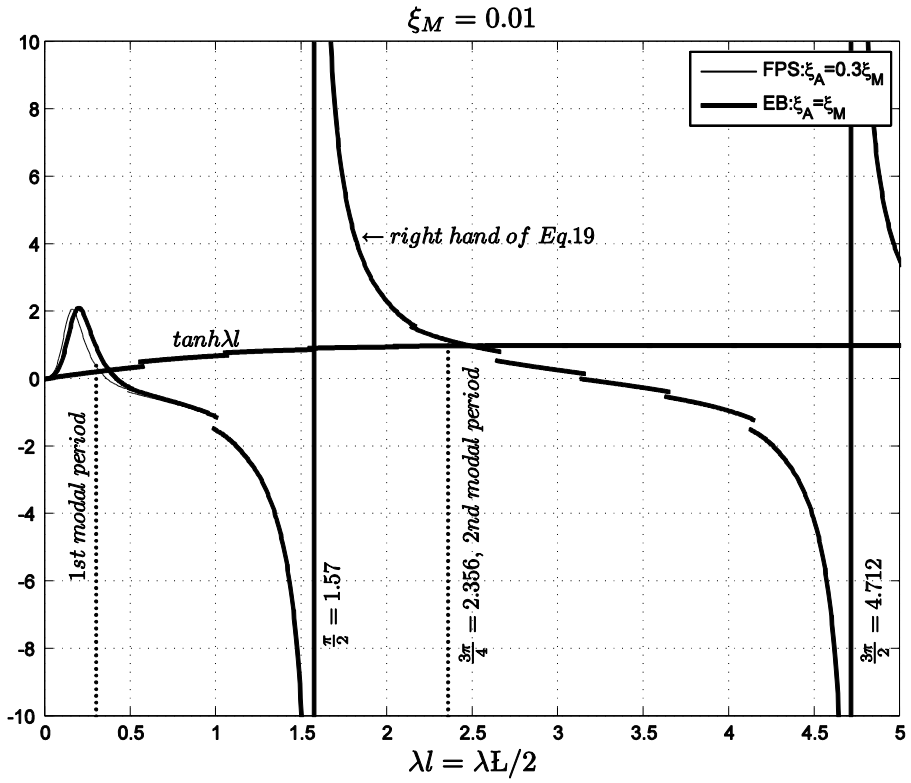

Fig. 6. Behavior of the right hand side of Equation (19) at the limiting cases of small values of ξ.

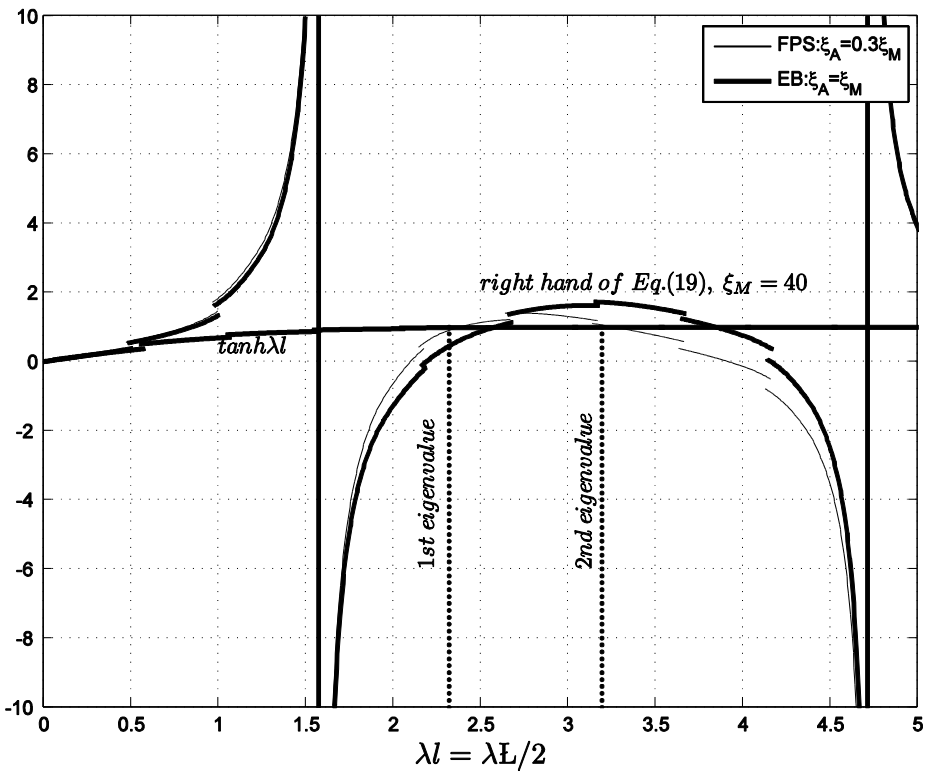

Fig. 7. Solution of the transcendental Equation (19).

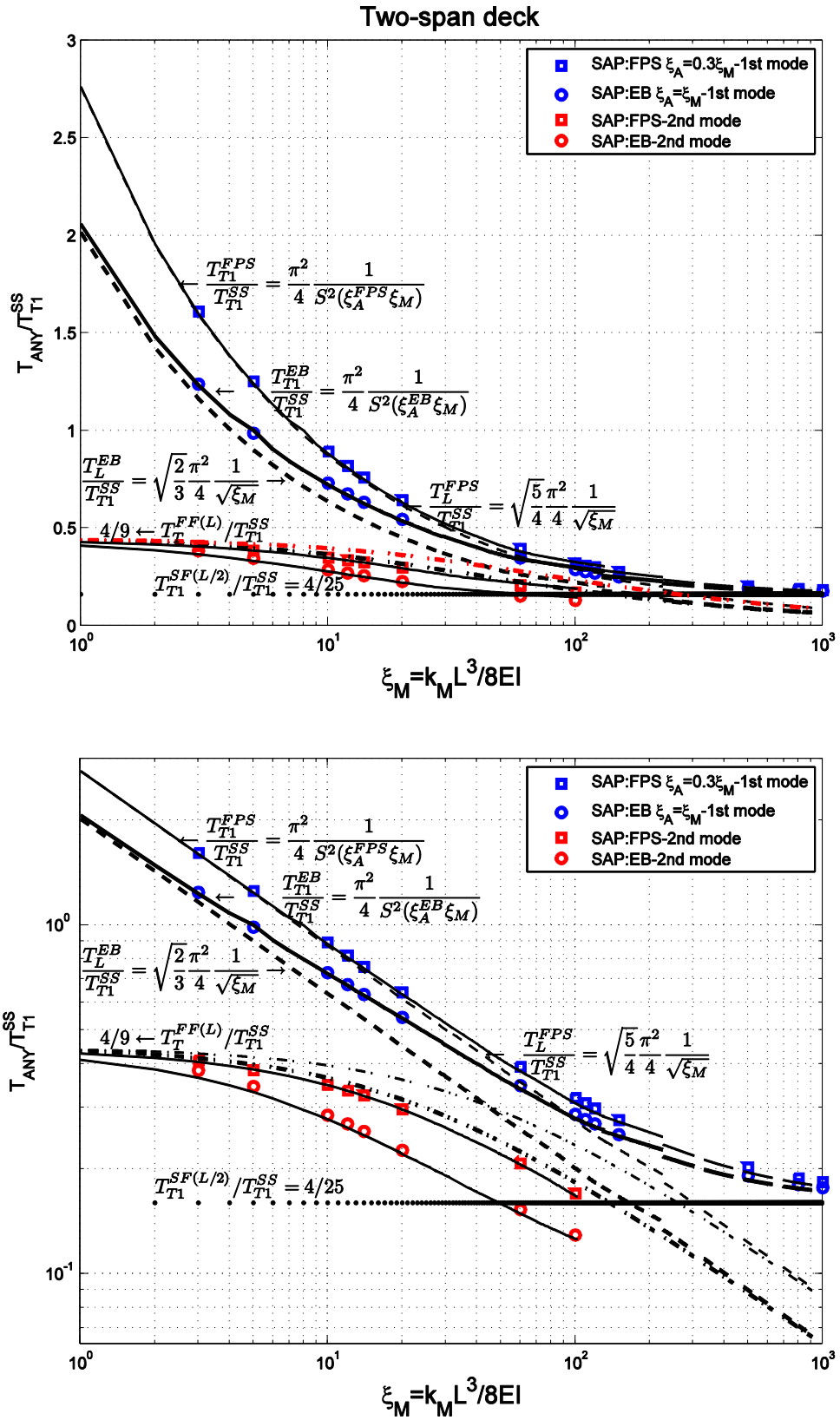

Fig. 8. Comparison of the normalized first and second transverse periods T_T of a two-span isolated deck of length L (solutions of Equation (19) given by the solid lines) against the longitudinal isolation periods T_L^{EB} or T_L^{FPS} (EB =Elastomeric Bearings, FPS =Friction Pendulum System) given by the dashed lines. Top:Semilog plot, Bottom:Logarithmic plot. Additional chain lines correspond to the transverse eigenperiods from an equivalent beam on Winkler foundation

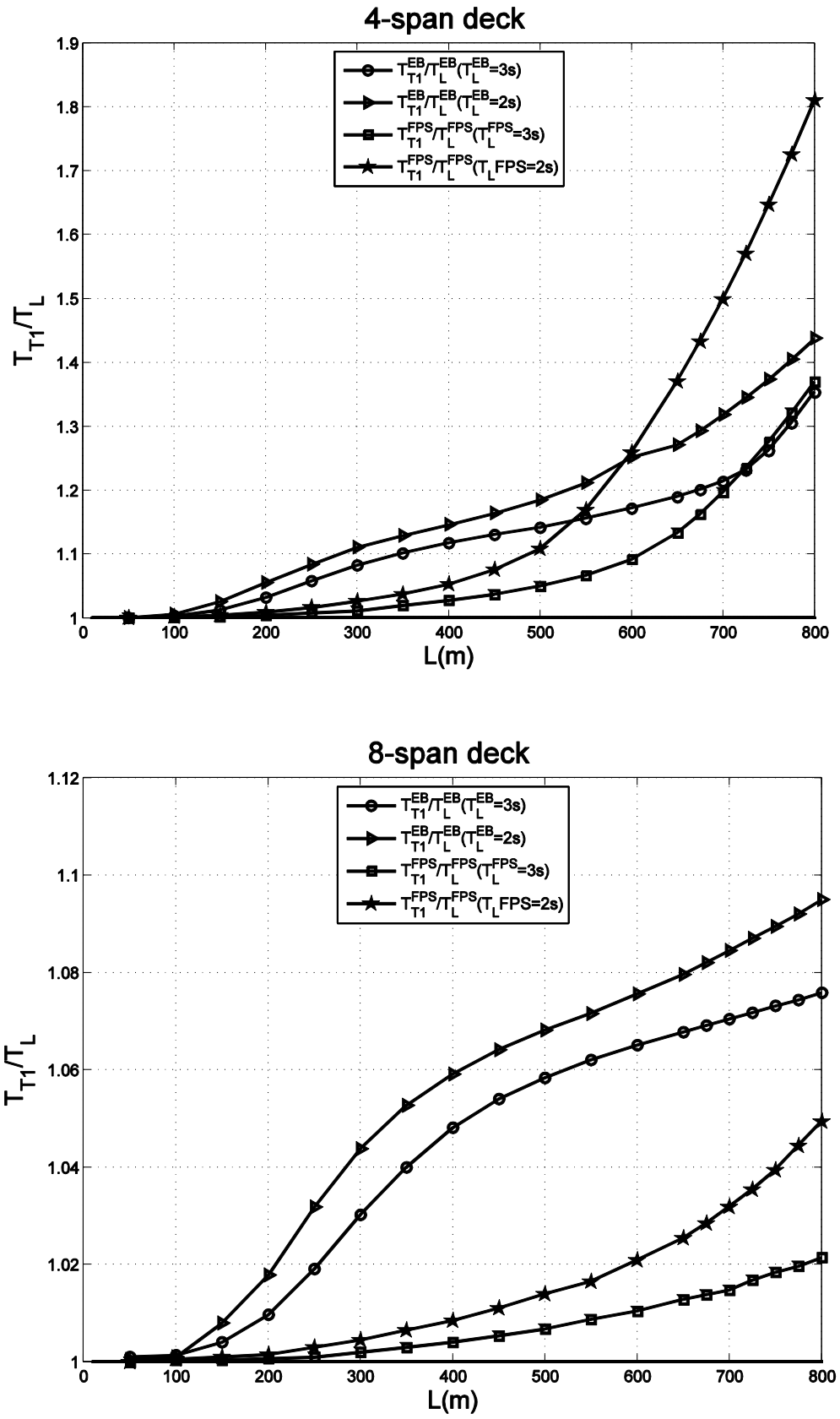

Fig. 9. First transverse period of a deck isolated either with elastomeric or spherical sliding bearings normalized to the longitudinal isolation period ($T_L = 2.0$ or 3.0 sec). Top: 4-span deck; Bottom: 8-span deck.

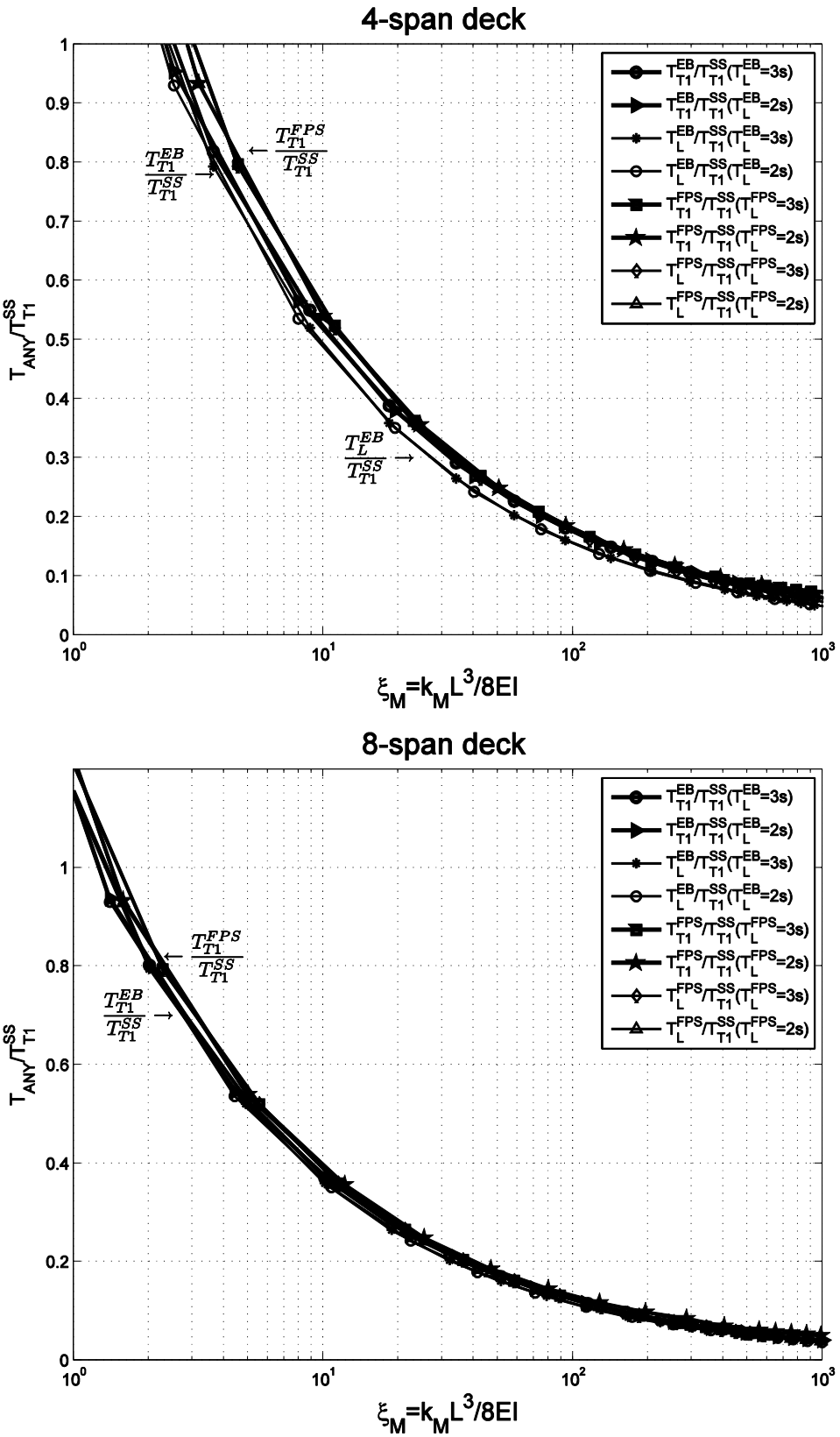

Fig. 10. Comparison of the master curve of the first transverse period T_{T1} of an isolated deck against the corresponding longitudinal isolation periods T_L^{EB} or T_L^{FPS} (EB =Elastomeric Bearings, FPS =Friction Pendulum System). Top: 4-span deck; Bottom: 8-span deck.

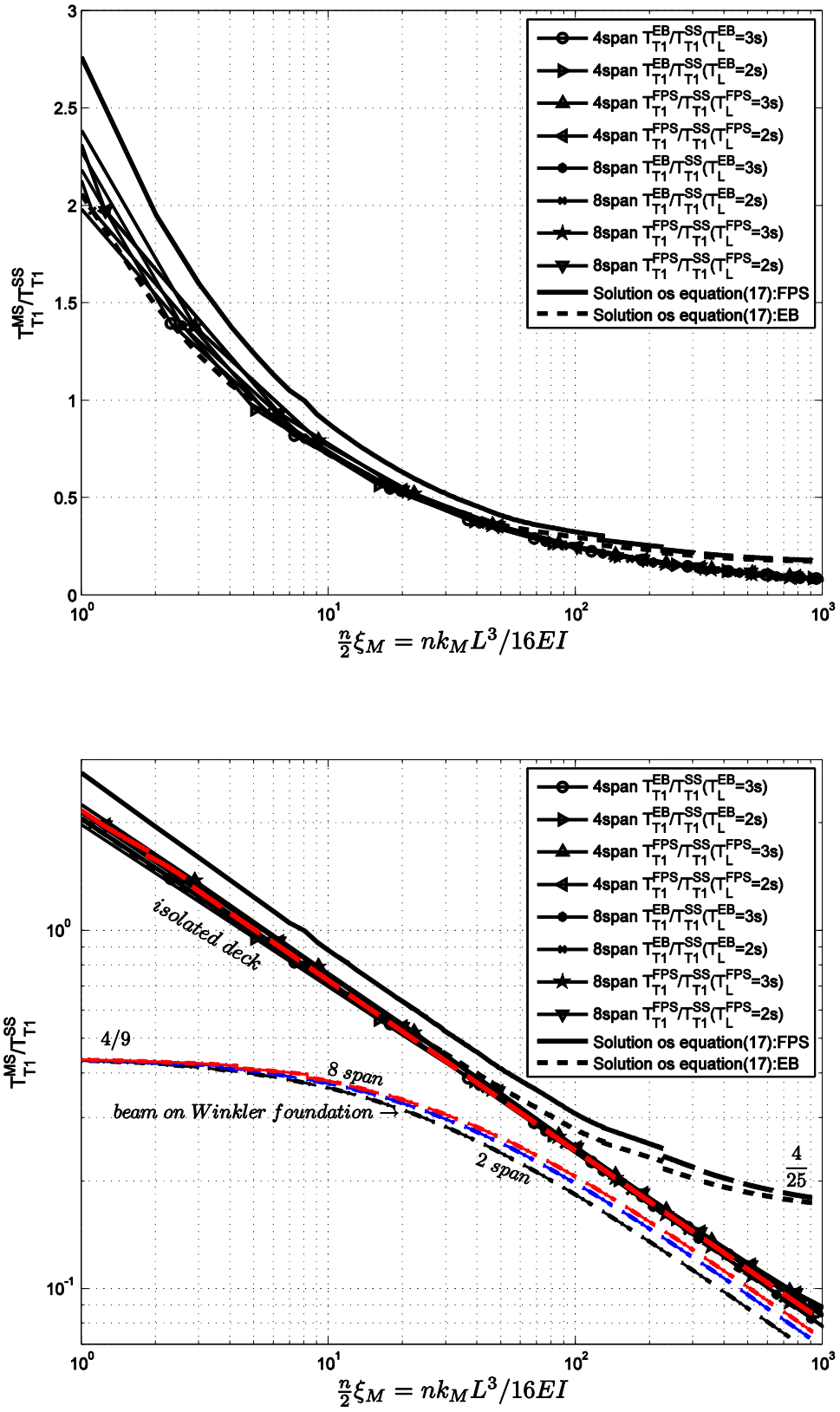

Fig. 11. Master Curve of the first transverse period of any multi-span isolated deck with arbitrary longitudinal isolation period; Top:Semilog plot, Bottom:Logarithmic plot, showing also the transverse periods obtained from the equivalent beam on Winkler foundation of a 2,4 and 8-span deck.